THE JOURNAL OF COMPARATIVE NEUROLOGY 329:36–52 (1993)

Frequency Organization of the Dorsal Cochlear Nucleus in Cats

GEORGE A. SPIROU, BRADFORD J. MAY, DEBORA D. WRIGHT, AND DAVID K. RYUGO
Center for Hearing Sciences, Departments of Otolaryngology-HNS and Neuroscience, Johns Hopkins University School of Medicine, Baltimore, Maryland 21205

ABSTRACT

Sensory epithelia are often spatially reiterated throughout their representation in the central nervous system. Differential expression of this representation can reveal specializations of the organism's behavioral repertoire. For example, the nature of the central representation of sound frequency in the auditory system has provided important clues in understanding ecological pressures for acoustic processing. In this context, we used electrophysiological techniques to map the frequency organization of the dorsal cochlear nucleus in nine cats. Frequency responses were sampled in increments of 100–200 μm along electrode tracks that entered the dorsomedial border of the nucleus and exited at the ventrolateral border. Electrode tracks were oriented parallel to the long (or strial) axis of the nucleus so that each penetration sampled neural responses for most of the cat's audible frequencies and remained in or near the pyramidal cell layer for several millimeters. Nearly identical distance versus frequency relationships were obtained for different rostral-caudal locations within the same cat as well as for different cats. Frequency responses systematically decreased from above 50 kHz at the most dorsomedial locations in the nucleus to below 1 kHz in the most ventrolateral regions. The rate of frequency change was roughly three times greater in high frequency regions than in low frequency regions. In addition, the highest pyramidal cell density and longest rostral-caudal axis was observed for the middle third of the dorsal-ventral axis of the nucleus. As a result, roughly half of all pyramidal cells responded to frequencies between 8–30 kHz. The representation of neural tissue for these frequencies may be related to the importance of spectral cues in sound localization.

Key words: auditory system, electrophysiology, hearing, horseradish peroxidase, single unit recording, tonotopy

A frequency-to-place transformation is performed within the organ of Corti that establishes a spatially organized neural representation of sound frequency (Bekesy, '60). This orderly sequence of frequency organization within neural structures is termed tonotopy and has been demonstrated to be a fundamental property of the central auditory nervous system (reviewed by Clopton et al., '74). Moreover, variations in tonotopic organization have corroborated anatomically differentiated subdivisions within individual structures (Rose et al., '59; Woolsey, '60; Aitkin and Webster, '72; Merzenich and Reid, '74) and have yielded insights into the localization of certain functions within the brain (Guinan et al., '72; Bruns and Schmieszek, '80; Konishi, '86; Suga, '88). These kinds of diversities that exist across species have revealed the influence of habitat and lifestyle on the evolution of auditory specializations (Masterton et al., '75; Pollak, '89).

Previous tonotopic maps of the dorsal cochlear nucleus (DCN) have revealed a high-to-low frequency progression along dorsal-to-ventral locations in the nucleus (Rose et al., '59). The electrode tracks used to produce these data, however, were relatively short and the nucleus was not thoroughly explored. In the present study, we used stereotaxic procedures and electrophysiological recordings to sample the distribution of frequency representation along the strial axis of the DCN in the cat. In many instances, multiple parallel electrode tracks were recovered that encompassed much of the DCN and spanned most of the audible frequency range. The observed tonotopic organization is consistent with the notion that there is an increase in the spatial representation of high frequency information rela-

Accepted November 6, 1992.

Dr. G.A. Spirou is now at the Department of Otolaryngology, West Virginia University School of Medicine, 2222 Health Sciences Center, Morgantown, WV 26506.

Address reprint requests to D.K. Ryugo, Center for Hearing Sciences, Johns Hopkins University School of Medicine, Traylor 510, 720 Rutland Ave., Baltimore, MD 21205.

tive to that of the cochlea and anteroventral cochlear nucleus (Ryugo and May, '93), and with the implied role of the DCN in determining the location of sound sources (Sutherland and Masterton, '92).

MATERIALS AND METHODS

Animal preparation and electrophysiological techniques

Methods for electrophysiological recording in the DCN of decerebrate cats have been previously described in detail (e.g., Spirou and Young, '91). Briefly, healthy cats, weighing between 2 and 4 kg, and having clean ears were anesthetized with xylazine (Rompun, 2 mg IM) followed by ketamine HCl (Ketaset, 75–100 mg IM). Supplemental doses of ketamine were administered as necessary to keep the animal areflexic during the preparatory surgery. Atropine (0.1 mg IM) was given to control secretions, a tracheotomy was performed, and an indwelling catheter was placed in the cephalic vein for the delivery of intravenous fluids. A fenestration was made in the parietal bone, the underlying dura was retracted, and forebrain tissue was aspirated to expose the rostral aspect of the superior colliculus. Decerebration was accomplished by aspirating transversely through the superior colliculus under visual control until the brainstem was transected.

The left bulla was ventilated by inserting a 60 cm length of PE tubing (1.4 mm ID). A stereotaxic mount was attached to the skull so that calibrated movements of the animal's head could be made (May et al., '91). Both ear canals were transected near the tympanic membrane and the head mounted in a stereotaxic apparatus with the tip of the nose tilted downward 37° from the horizontal plane. A hollow ear bar served as a speculum for delivering calibrated acoustic stimuli (Sokolich, '77).

The cerebellum was exposed by removing the occipital and posterior parietal bones, and then aspirated until the dorsomedial limit of the DCN was revealed. The recording electrode was aligned 37° off the midsagittal plane and 37° off the coronal plane (see Fig. 1) to penetrate the DCN near its dorsomedial tip (at the 40–50 kHz region) and to remain within the nucleus for most of the length of its long axis.

Recording criteria

Both tungsten and platinum-iridium electrodes were used for recording physiological activity. The characteristic frequency (CF, that frequency to which the unit is most sensitive) and CF threshold (the lowest sound pressure level to which a CF tone evokes an auditory response) were determined using audiovisual criteria as the electrode was advanced in increments of 100–200 μm with the aid of a hydraulic micromanipulator. Typically, recordings were made at a minimum interval of 100 μm in order to avoid recording from the same unit twice. Recordings were classified as single unit, multi-unit, or tone hash. The single unit category contained units with action potentials that could be clearly isolated on the basis of their amplitude and wave form. The multiunit category consisted of several action potentials of variable but inseparable amplitudes. The tone hash category was used to describe those cases where tone burst stimulation resulted in a time-locked increase in the amplitude of the signal from the electrode but action potentials could not be isolated. Tone hash was typical of recordings from layer I of the DCN. At the conclusion of each electrode track, electrolytic lesions (5–10 μA of negative current for 10 seconds) were placed at defined frequency locations near the ventral and dorsal extremes of the nucleus sampled by the recording electrode. The lesions served as references for relating frequency measures to anatomical reconstruction data.

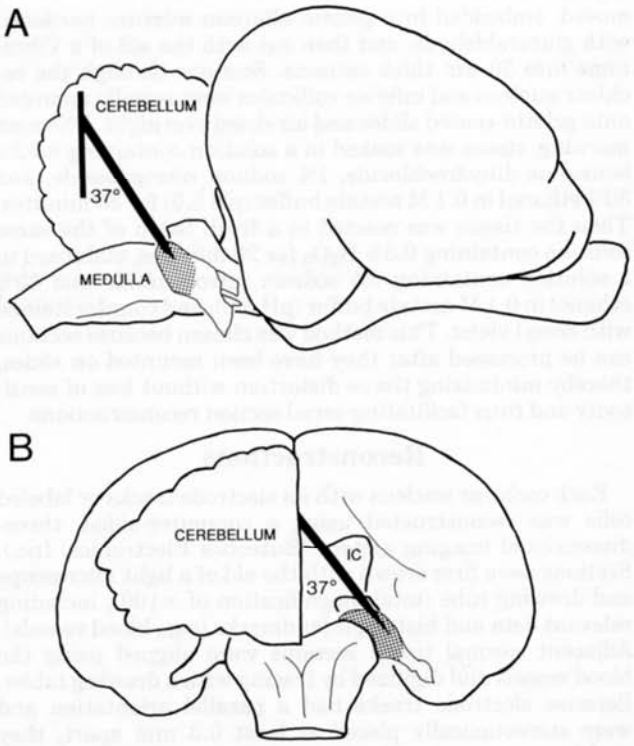

Fig. 1. Orientation of the electrode track in the brain as seen from a lateral (**A**) and caudal (**B**) view. Stereotaxic coordinates were used to guide the microelectrodes along the strial axis of the dorsal cochlear nucleus (shaded region). The right half of the cerebellum has been removed in this diagram. IC, inferior colliculus.

Histological processing

At the end of each physiological experiment, the animal was administered a lethal dose of Nembutal, placed on a respirator, and then transcardially perfused with 100 ml of a solution containing 0.5% sodium nitrite in 0.1 M phosphate-buffered saline (pH 7.3) followed immediately by 1.5 liters of a solution containing 2% paraformaldehyde and 2% glutaraldehyde in 0.1 M phosphate buffer (pH 7.3). The brain was postfixed in the same fixative for 24 hours, removed from the skull, cryoprotected in 10%, 20%, and 30% sucrose solutions, and sectioned parallel to the electrode tracks with the aid of a freezing microtome. Serial, 48 μm sections were collected, mounted on gelatin-coated slides, and stained with 0.5% cresyl violet.

In the case of cell labeling experiments, a microliter syringe loaded with 30–40% horseradish peroxidase (HRP, Sigma Chemical Co., St. Louis, MO, type VI) in 0.1 M Tris buffer (pH 7.6) was mounted on a micromanipulator and advanced into the inferior colliculus in three sites, separated by several millimeters in the anterior-posterior direction. A total of 1 μL was injected along each track. Roughly 24 hours after these injections, the animal was given a lethal dose of Nembutal and immediately perfused using the above mentioned procedure. The brain stem was re-

moved, embedded in a gelatin-albumin mixture hardened with glutaraldehyde, and then cut with the aid of a Vibratome into 50 μm thick sections. Sections through the cochlear nucleus and inferior colliculus were serially mounted onto gelatin-coated slides and air-dried overnight. The next morning, tissue was soaked in a solution containing 0.02% benzidine dihydrochloride, 1% sodium nitroprusside, and 30% ethanol in 0.1 M acetate buffer (pH 5.0) for 30 minutes. Then the tissue was reacted in a fresh batch of the same solution containing 0.3% H_2O_2 for 20 minutes, stabilized in a solution containing 3% sodium nitroprusside and 50% ethanol in 0.1 M acetate buffer (pH 5.0), and counterstained with cresyl violet. This method was chosen because sections can be processed after they have been mounted on slides, thereby minimizing tissue distortion without loss of sensitivity and thus facilitating serial section reconstructions.

Reconstructions

Each cochlear nucleus with its electrode tracks or labeled cells was reconstructed using a computer-aided, three-dimensional imaging system (Eutectics Electronics, Inc.). Sections were first drawn with the aid of a light microscope and drawing tube (total magnification of ×100), including relevant data and histologic landmarks (e.g., blood vessels). Adjacent coronal tissue sections were aligned using the blood vessels and digitized by tracing with a drawing tablet. Because electrode tracks had a parallel orientation and were stereotaxically placed at least 0.3 mm apart, they could be recovered with high confidence. The similarity of each computer-generated image of the reconstructed DCN compared to its appearance prior to sectioning provided evidence for the reliability of the reconstruction method. The reconstructed nucleus could then be arbitrarily rotated about any axis and viewed with respect to the electrode tracks and/or DCN layer.

RESULTS

The present results are based on the electrophysiological and anatomical observations made in 12 cats. In nine animals, physiological recordings were correlated with the complete reconstructions of electrode tracks. The objective of the physiological study was to relate frequency responses of single and multiple units to their anatomic position in the nucleus, with special attention paid to individual cellular layers and the cellular constituents of the DCN. In three other animals, HRP was extracellularly injected into one inferior colliculus and analysis of HRP-labeled pyramidal cells in the contralateral DCN was made. The objective of the cell labeling study was to investigate the relationship between pyramidal cell density and frequency representation in the nucleus.

Electrode track analysis

Under a light microscope, the presence of an electrode track was marked by tears in the tissue, gliosis, extravascular erythrocytes, and a pair of lesion sites (Fig. 2A). Lesion sites were characterized by a hole in the tissue surrounded by an extra dense accumulation of glial cells. Because only a few electrode penetrations were made in any nucleus, the identity of each track was based on its relative anterior-posterior position and spatial orientation within the nucleus. The identification was corroborated by the microdrive readings as they correlated to the position of the site of entry of the electrode, by the position and frequency characteristics of the lesion sites, and by the distance between lesion sites. Because the CF at each lesion site was determined prior to the electrocoagulation, lesions could serve as reference points for the assignment of recording loci along the electrode track and permit compensation for hysteresis in the microdrive and/or dragging of tissue by the electrode as it was moved.

At each recording site along an identified electrode track, the distance traversed with respect to initial contact with the tissue surface was registered. Lesion sites could then be assigned a position along the frequency-distance plot on the basis of their CF. Then, the distance between lesions as registered by the microdrive was proportionally scaled with respect to the lesion sites as recovered in histological tissue sections. In this manner, each recording site could be assigned a position along the electrode track (Fig. 2B) and analyzed with respect to the neural tissue.

Organization of frequency along the strial axis

There was a systematic relationship between the location of the recording site and the frequency response characteristics at that site. As the electrode passed from dorsal to ventral along the strial axis of the DCN, neurons exhibited progressively lower CFs. This general tonotopic sequence has been previously described (Rose et al., '59), but our electrode tracks were specifically aimed along the strial axis and remained in the nucleus for 3–5 mm, thereby providing a more complete picture of the frequency organization of the DCN. The distance versus frequency plot revealed a relatively smooth transition of frequencies and an increasing slope with increasing frequency (Fig. 2C). It is also noteworthy that there are no abrupt transitions in the plot with respect to the degree of unit isolation or the layer crossings by the electrode (Fig. 3). Our descriptions of this frequency organization encompass most of the audible hearing range for cats (Heffner and Heffner, '85).

Organization of frequency along the rostral-caudal axis

Recording tracks were placed in different rostral-caudal sectors of the DCN, so that the frequency organization could also be investigated across the strial axis of the nucleus (Fig. 4). Each track tended to be oriented within the plane of the histologic tissue section (Fig. 5), and so could be assigned a percentile location by referencing the section number containing the track to the total number of sections spanning the nucleus (0% was the caudal tip and 100% was the rostral pole of the DCN). When a least squares fit was used to superimpose individual distance versus frequency plots, the shapes of the plots for different sectors of a single nucleus were virtually identical (Fig. 4).

This tonotopic organization proved reliable across separate cats and without regard to their quartile location (Fig. 6A–D). The scatter of points is relatively small, emphasizing the similarity of frequency representation within similar regions of the nucleus. In the rostral quartile, there was one track at 75.5% (open circles) and another at 84% (filled circles). The track at 75.5% was similar to all tracks located more caudally, and it encompasses approximately the same frequency range. The most rostral track traversed the shortest distance in our sample and consequently encountered a limited frequency range. Nevertheless, the shorter distance corresponds to a narrowing of the nucleus in this rostral quartile, and the shape of the truncated plot is still congruent with the corresponding frequency regions of the

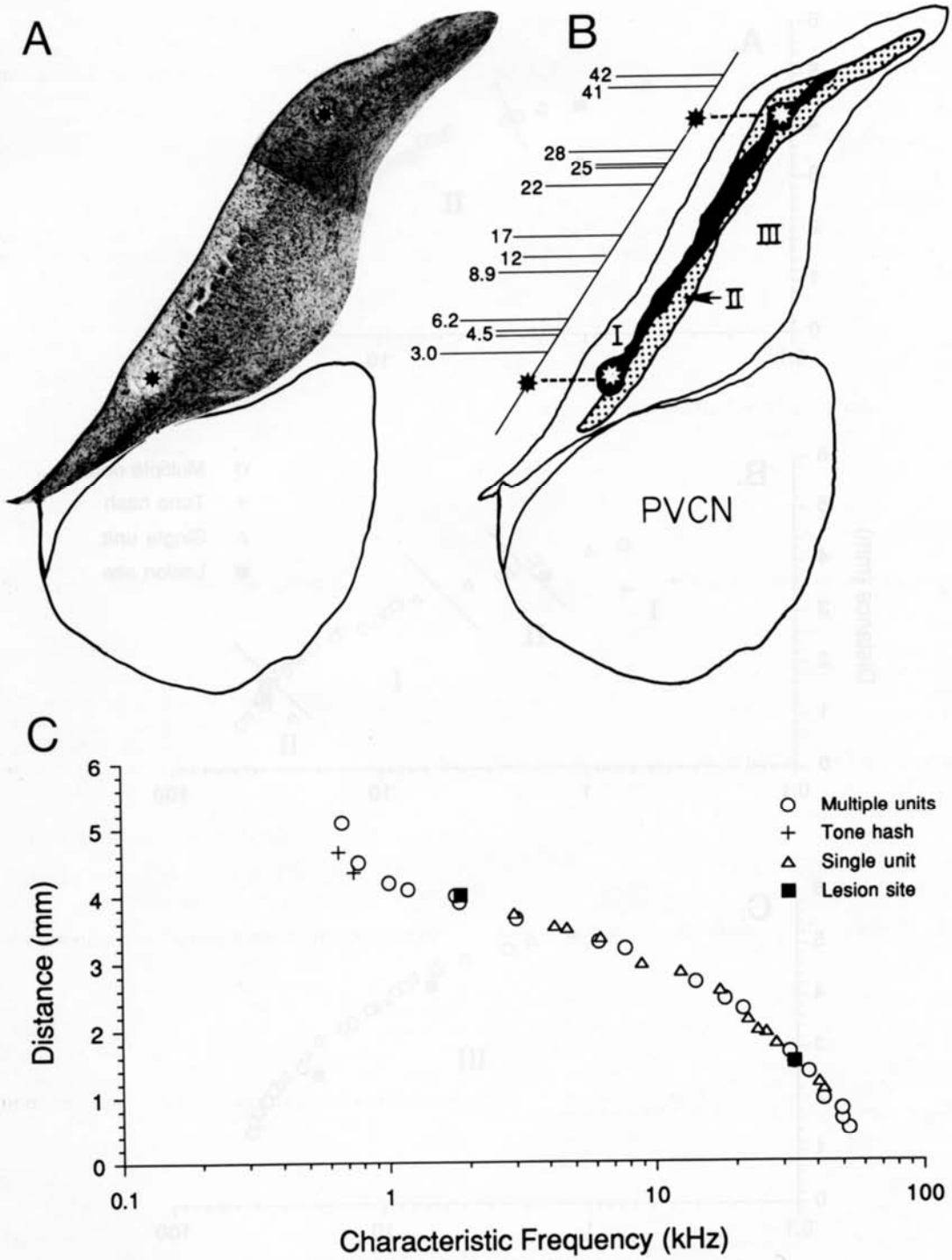

Fig. 2. Distribution of frequency along the strial axis of the DCN. (**A**) Photomicrograph of transverse section through the DCN, illustrating the tissue damage along an electrode track and the electrolytic lesions (marked by asterisks). (**B**) Drawing of this same section, showing the position of the track (black) and lesion sites (asterisks) with respect to layer II of the DCN (stipple). Single unit locations and CFs are indicated to the left. Roman numerals indicate the layer. PVCN, posteroventral cochlear nucleus. (**C**) Frequency determinations at regular intervals along the electrode track demonstrate a progressive and systematic decrease in CF with distance traversed, independent of the degree of unit isolation.

others. A composite plot containing all data points was created (Fig. 6E), which demonstrates that the strial distance between similar frequency points was remarkably constant throughout the DCN, despite variations in nuclear size and shape, recording quartile and layer within the nucleus, or absolute angle of the electrode track.

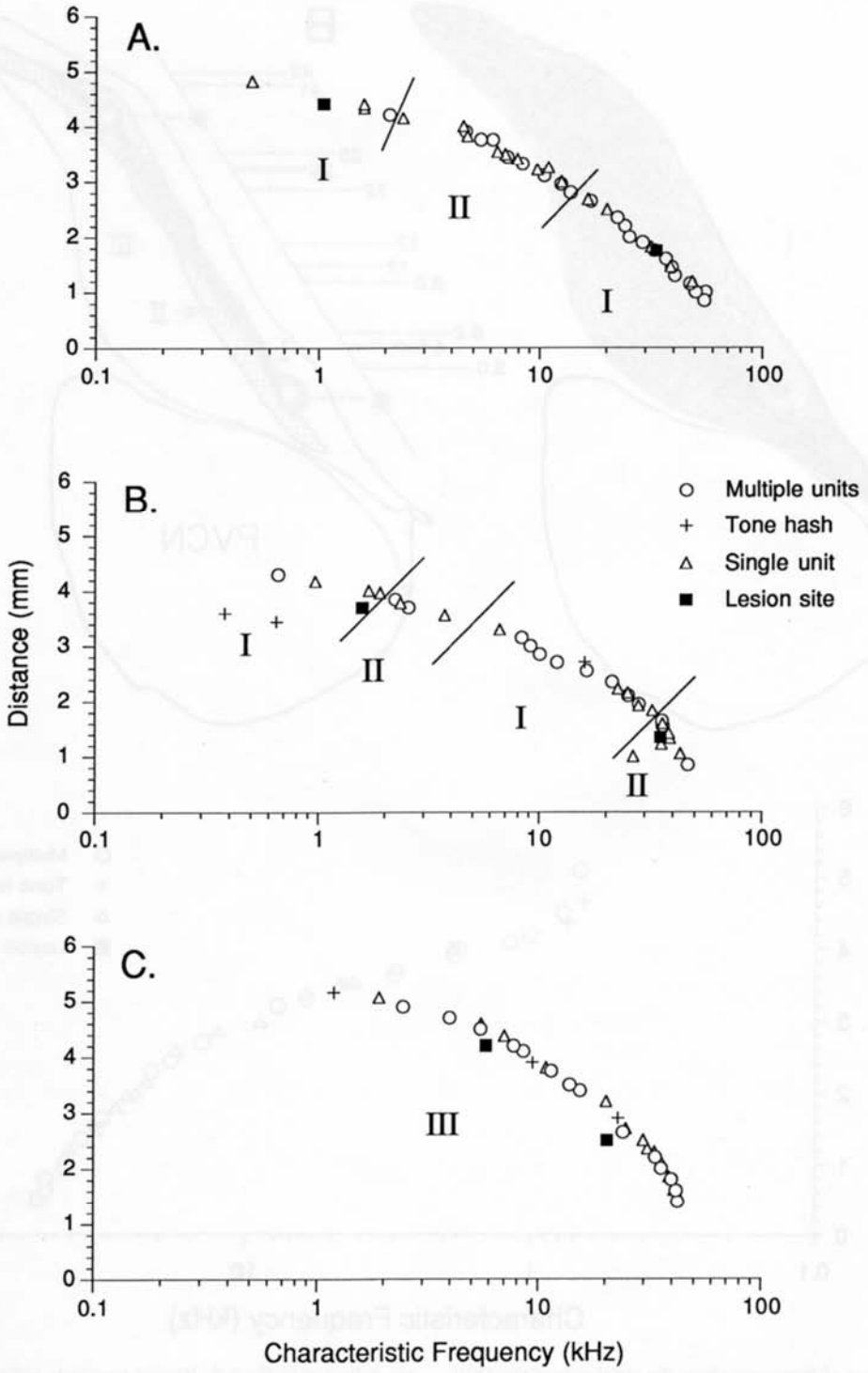

Fig. 3. Distance versus frequency plots for three separate cats (**A–C**). Lines indicate the location of the layer crossing and Roman numerals indicate the layer. There are no abrupt shifts in the frequency plots when the electrode passes from one layer to the next.

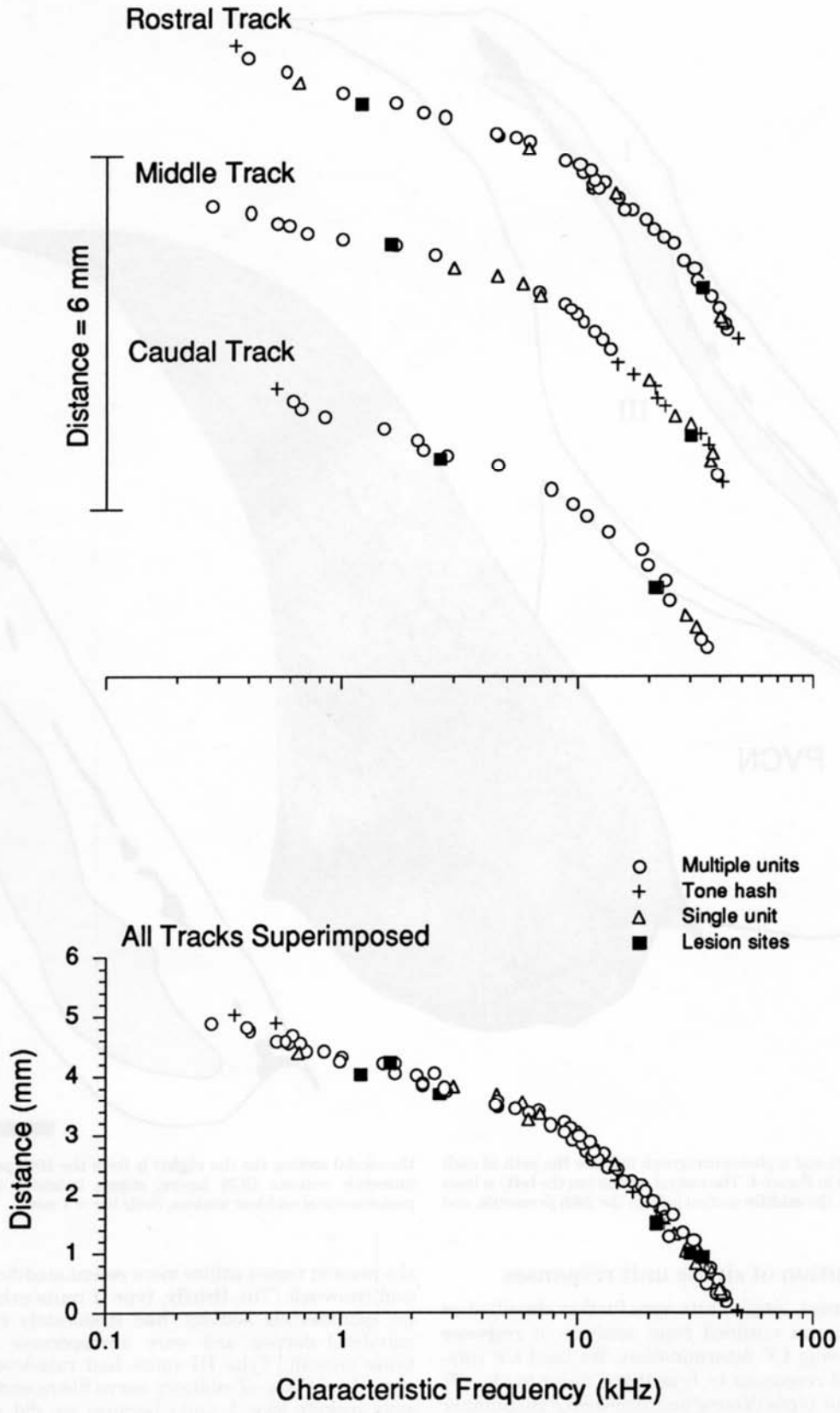

Fig. 4. Distance versus frequency plots from three separate rostral-caudal locations from a single DCN. Note that the frequency plots have a very similar profile despite their differences in location.

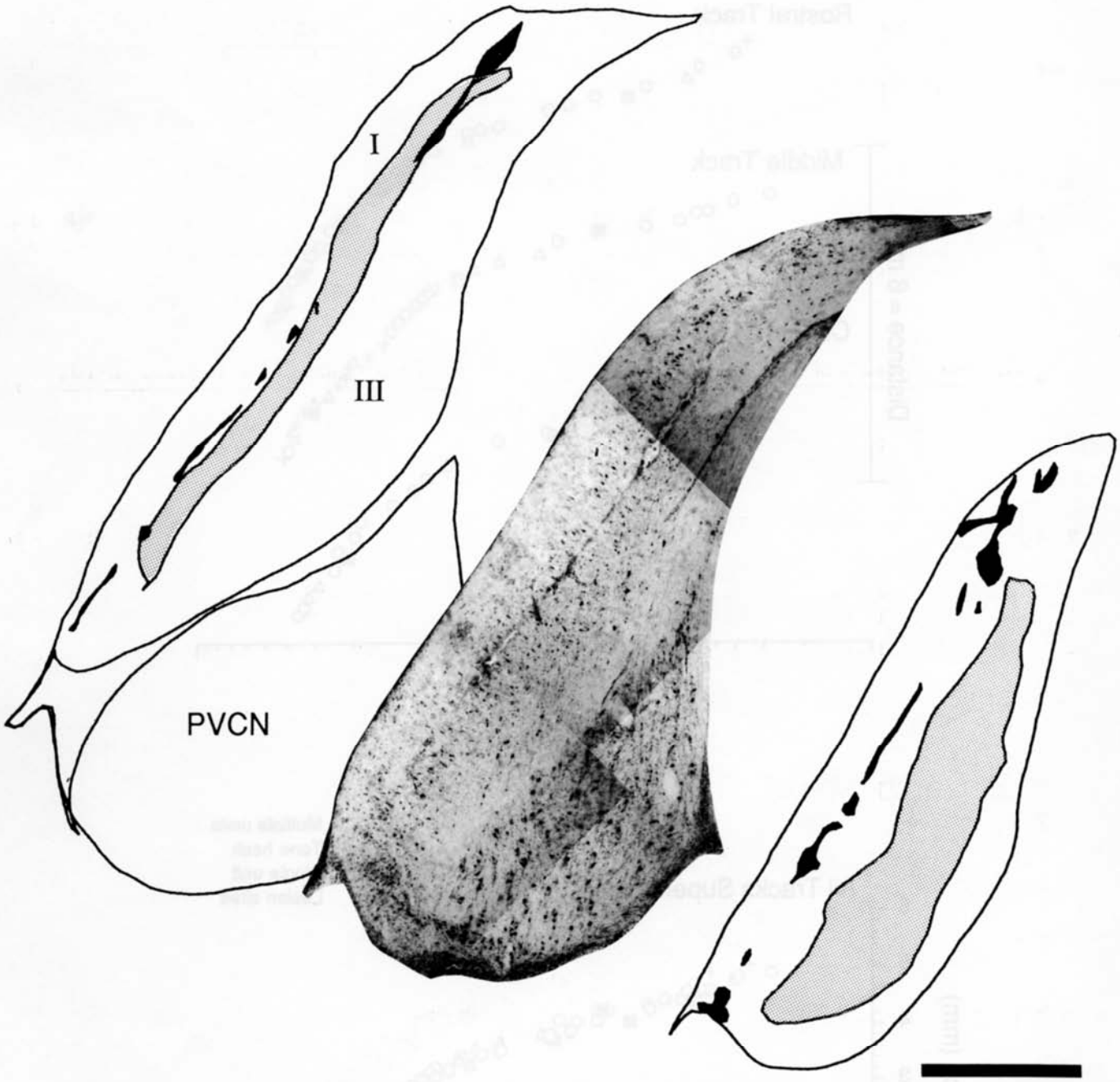

Fig. 5. Drawings and a photomicrograph indicate the path of each track (black) shown in Figure 4. The rostral section (on the **left**) is from the 49th percentile, the **middle** section is from the 29th percentile, and the caudal section (on the **right**) is from the 10th percentile. Roman numerals indicate DCN layers; stipple indicates layer II; PVCN, posteroventral cochlear nucleus. Scale bar = 1 mm.

Distribution of single unit responses

In some instances, single units were further classified on the basis of criteria outlined from analysis of response properties following CF determination. We used CF rate-level curves and responses to broadband noise to classify the data into unit types (Young and Brownell, '76; Shofner and Young, '85). Unit categories in unanesthetized cats were originally defined on the basis of response map features (Evans and Nelson, '73), but the criteria used in the present report utilize more recent modifications (Young and Brownell, '76). Briefly, type II units exhibited little or no spontaneous activity, had moderately non-monotonic rate-level curves, and were unresponsive to broadband noise stimuli. Type III units had rate-level curves that resembled those of auditory nerve fibers and in this report may include type I units because we did not verify the presence of inhibitory sidebands. Type IV units gave excitatory responses to CF tones at sound levels near threshold but stopped responding to CF tones at higher sound levels.

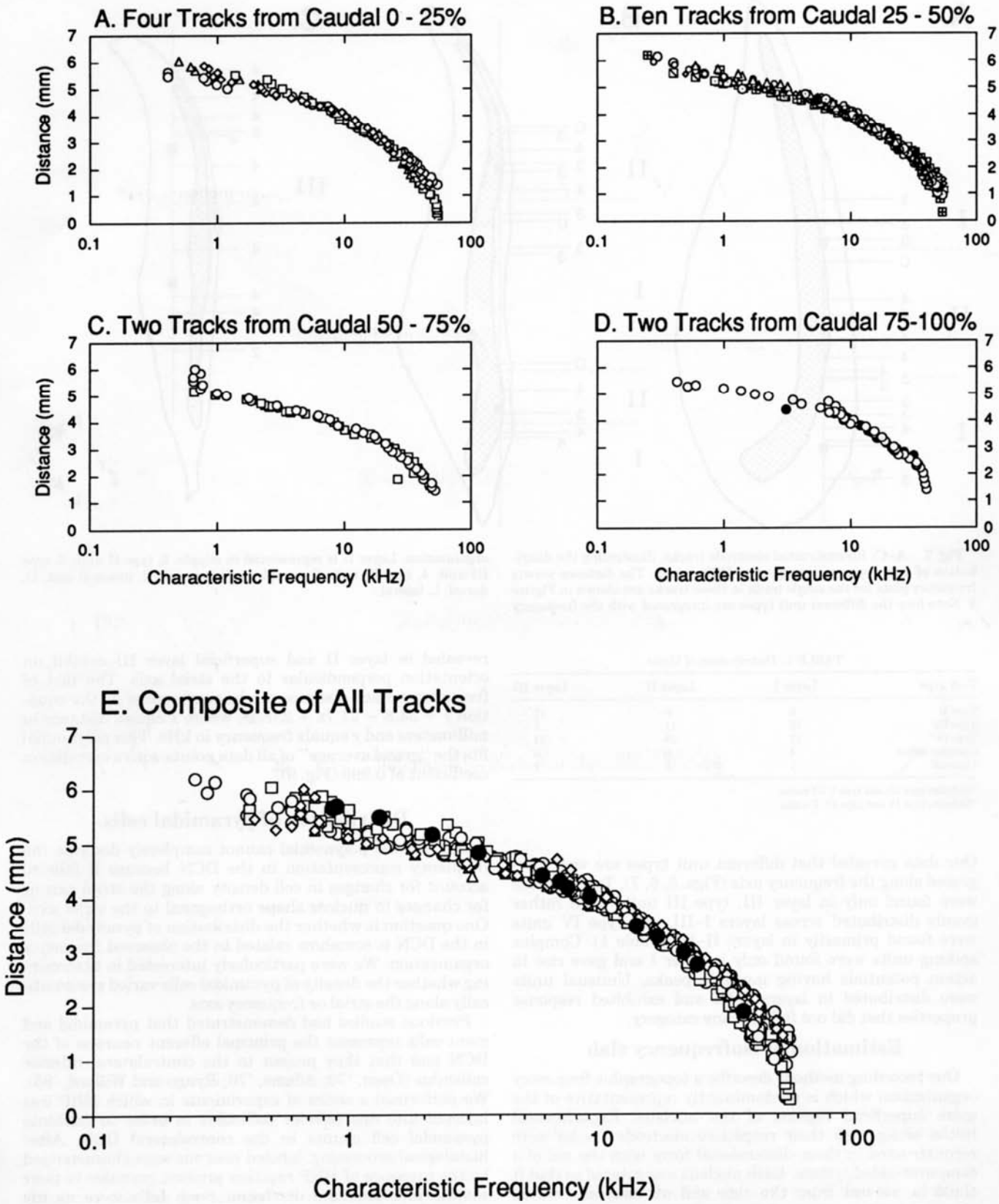

Fig. 6. Distance versus frequency plots for all cats grouped by quartile location along the rostral-caudal axis of the DCN (**A–D**). Plots from the same and different quartiles, and from different cats exhibit the same frequency organization when plotted together (**E**). The filled circles represent recording sites from an electrode track shown in Figure 7.

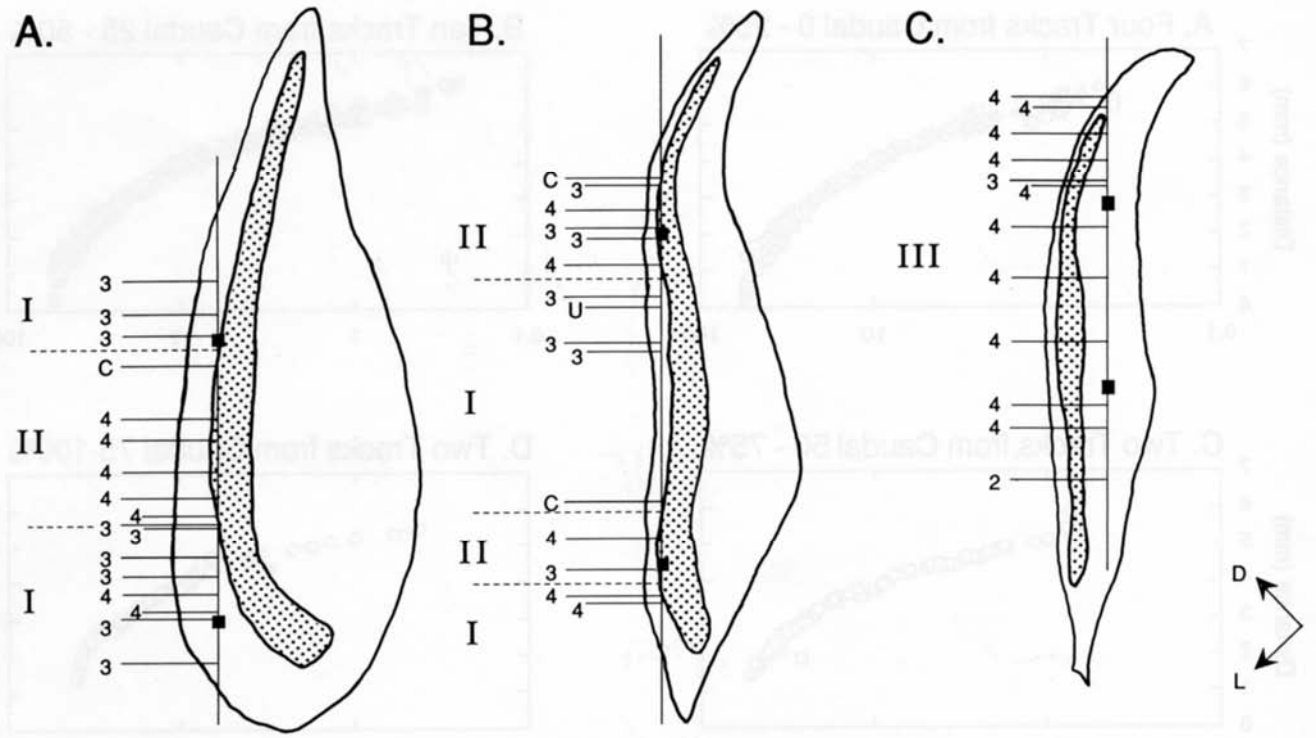

Fig. 7. **A–C:** Reconstructed electrode tracks, illustrating the distribution of unit types with respect to DCN layers. The distance versus frequency plots for the single units in these tracks are shown in Figure 3. Note how the different unit types are integrated with the frequency organization. Layer II is represented in stipple. 2, type II unit; 3, type III unit; 4, type IV unit; C, complex spiking unit; U, unusual unit; D, dorsal; L, lateral.

TABLE 1. Distribution of Units

Unit type	Layer I	Layer II	Layer III
Type II	0	0	17
Type III[1]	10	11	7
Type IV[2]	12	28	24
Complex spikes	4	0	0
Unusual	1	3	2

[1]Includes type III and type I/III units.
[2]Includes type IV and type IV-T units.

Our data revealed that different unit types are well integrated along the frequency axis (Figs. 3, 6, 7). Type II units were found only in layer III, type III units were rather evenly distributed across layers I–III, and type IV units were found primarily in layers II–III (Table 1). Complex spiking units were found only in layer I and gave rise to action potentials having multiple peaks. Unusual units were distributed in layers I–III and exhibited response properties that did not fall into any category.

Estimation of isofrequency slab

Our recording methods describe a topographic frequency organization which is predominantly representative of the more superficial regions of the nucleus. Experimental nuclei along with their respective electrode tracks were reconstructed in three-dimensional form with the aid of a computer-aided system. Each nucleus was rotated so that it could be viewed from the side and all electrode tracks visualized. Then, points of similar frequencies within layer II were connected and isofrequency contours defined (Fig. 8). These data indicate that the isofrequency contours revealed in layer II and superficial layer III exhibit an orientation perpendicular to the strial axis. The plot of frequency versus distance can be represented by the equation $y = 54.8 - 21.7x + 2.09x^2$, where x equals distance in millimeters and y equals frequency in kHz. This polynomial fits the "grand average" of all data points with a correlation coefficient of 0.999 (Fig. 9).

Distribution of pyramidal cells

Our derived polynomial cannot completely describe the frequency representation in the DCN because it fails to account for changes in cell density along the strial axis or for changes in nuclear shape orthogonal to the strial axis. One question is whether the distribution of pyramidal cells in the DCN is somehow related to the observed frequency organization. We were particularly interested in determining whether the density of pyramidal cells varied systematically along the strial or frequency axis.

Previous studies had demonstrated that pyramidal and giant cells represent the principal efferent neurons of the DCN and that they project to the contralateral inferior colliculus (Osen, '70; Adams, '79; Ryugo and Willard, '85). We performed a series of experiments in which HRP was injected into one inferior colliculus in order to facilitate pyramidal cell counts in the contralateral DCN. After histological processing, labeled neurons were characterized by the presence of HRP reaction product granules in their somata and proximal dendrites. Such cells were mostly confined to layer II but were also found scattered along the deep border of the nucleus (Figs. 10, 11). Labeled neurons were clearly larger than the unlabeled neuron population.

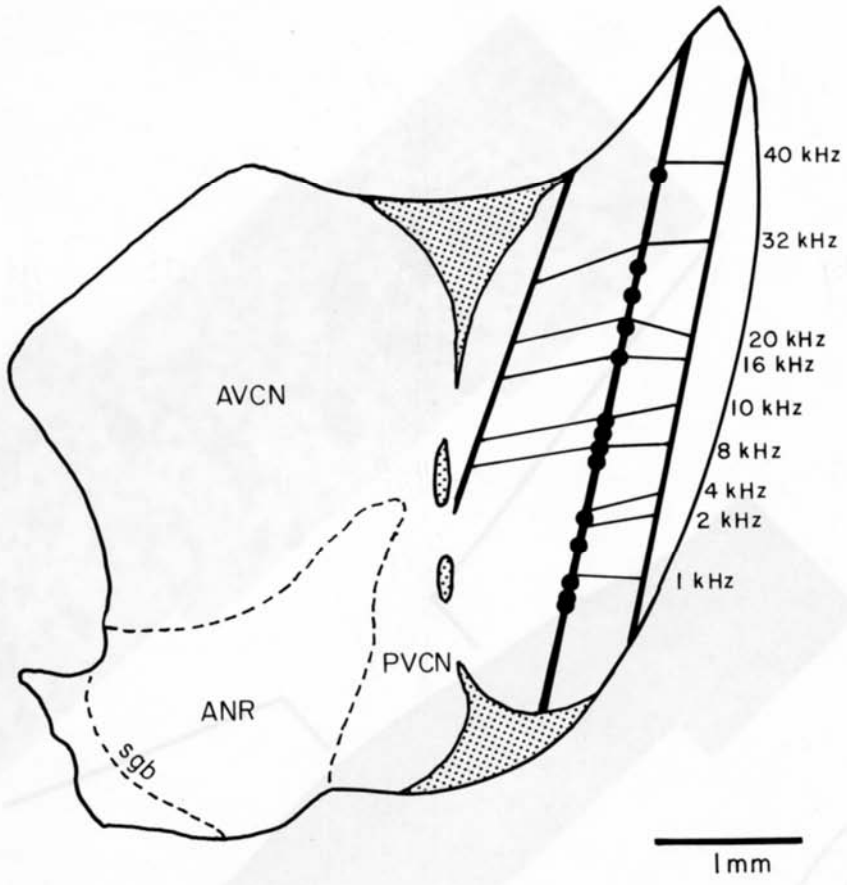

Fig. 8. Orientation of isofrequency laminae (or contours) within the DCN. Laminae for a representative set of frequencies were determined by interpolating the location of each frequency on three parallel tracks, and then connecting matching frequency sites with straight lines. The resulting laminae are oriented perpendicular to the strial axis of the DCN. Filled symbols along the middle track indicate the location of single unit responses shown in Figure 5E. Stipple represents granule cell domains helping to mark the boundary between the VCN and the DCN. ANR, auditory nerve root; AVCN, anteroventral cochlear nucleus; PVCN, posteroventral cochlear nucleus; sgb, Schwann-glial border.

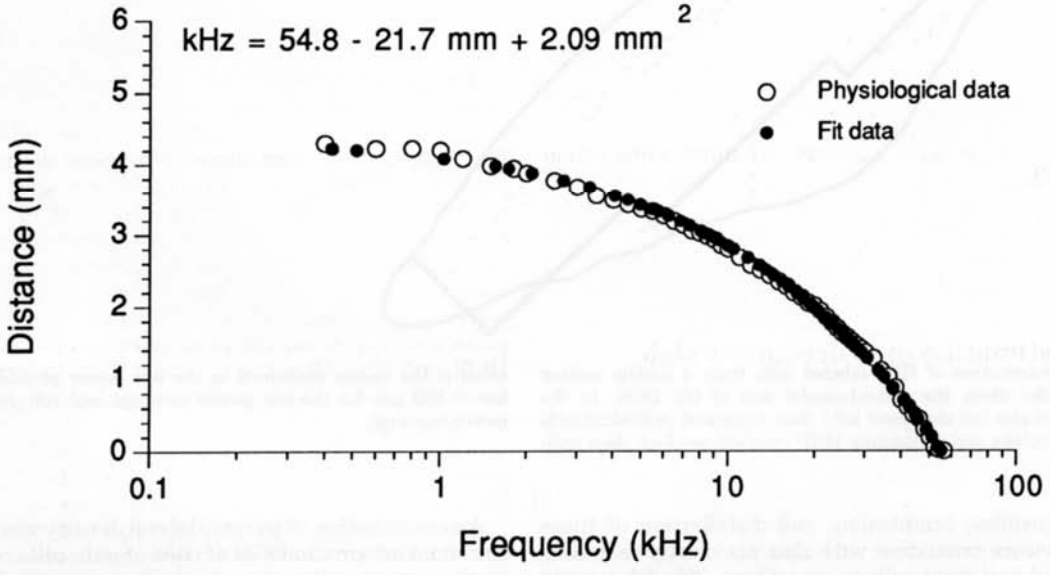

Fig. 9. A mathematical description of the frequency map for the DCN. Data computed from the second-order polynomial (filled symbols) produced an excellent fit (r = 0.999) to physiological data (open symbols).

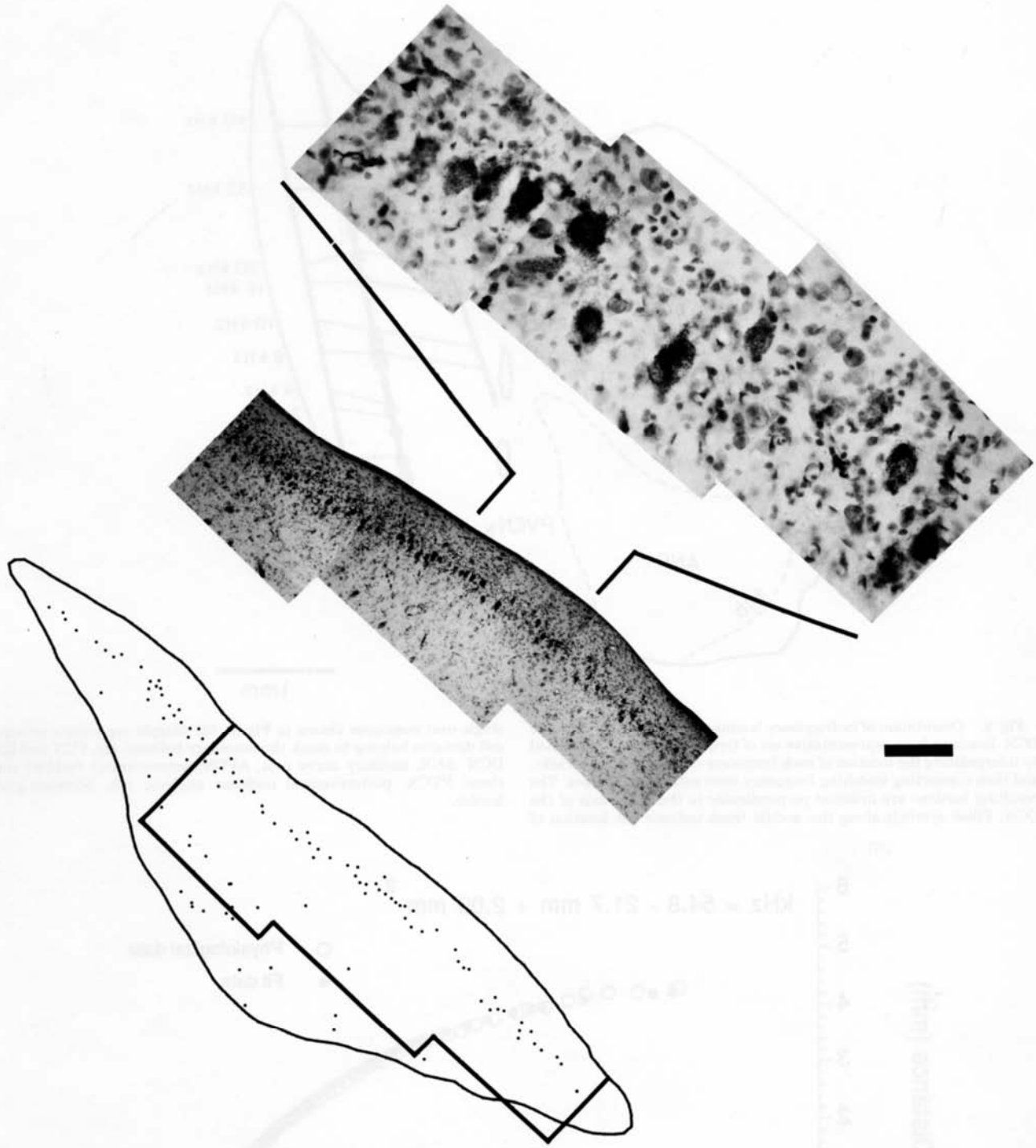

Fig. 10. Distribution of HRP-labeled cells from a middle section (50th percentile) along the rostral-caudal axis of the DCN. In the computer-aided plot (on the lower left), dots represent individual cells exhibiting a nucleus and containing HRP reaction product. Also indicated is the region contained in the low power photomontage. Scale bar = 500 μm for the low power montage and 100 μm for the high power montage.

The shape profiles, orientation, and distribution of these labeled cells were consistent with that previously described for pyramidal and giant cells in cats (Osen, '69; Adams and Warr, '76).

An examination of pyramidal cell density was made along the strial axis in the DCN of several animals, some of which were normal and some of which contained HRP-labeled neurons. In all HRP cases, the location of labeled cells was

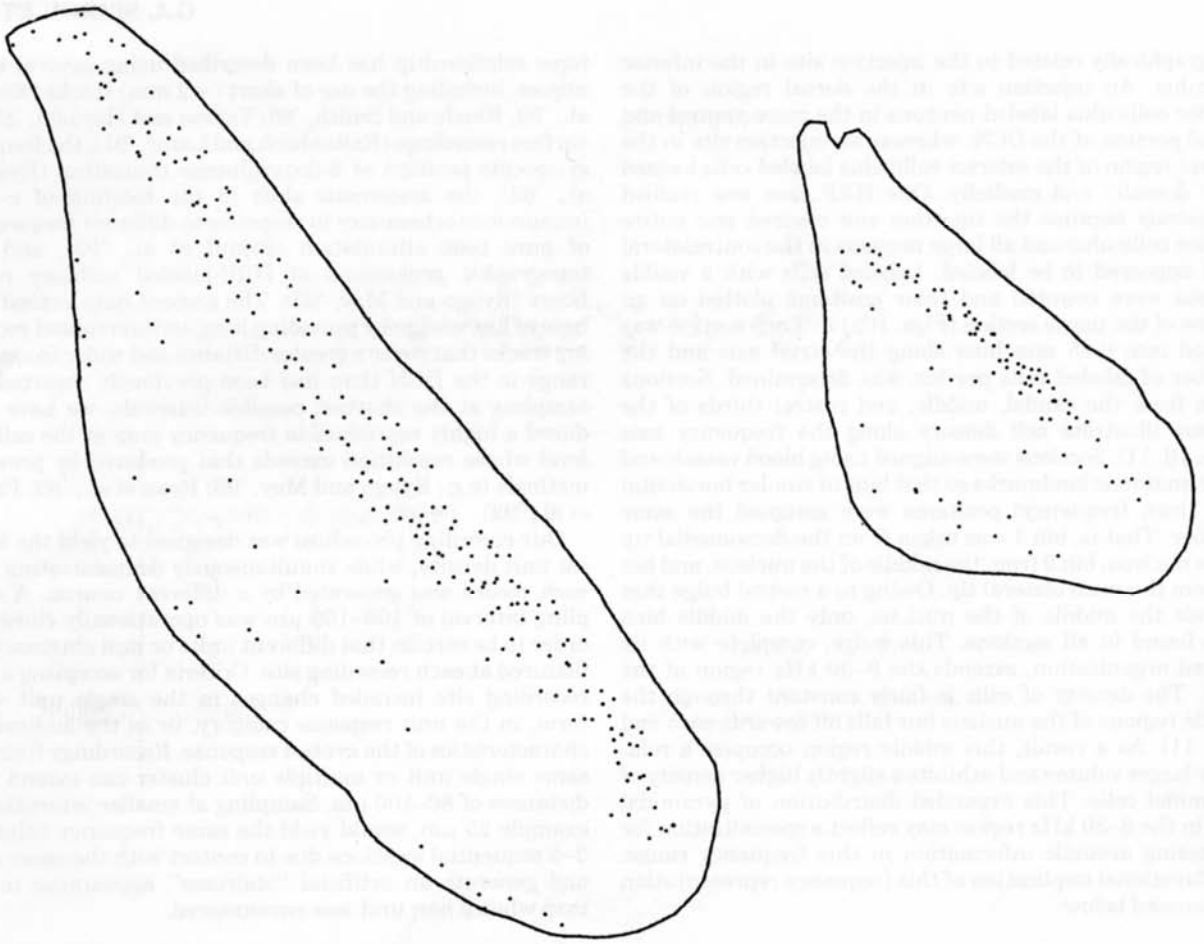

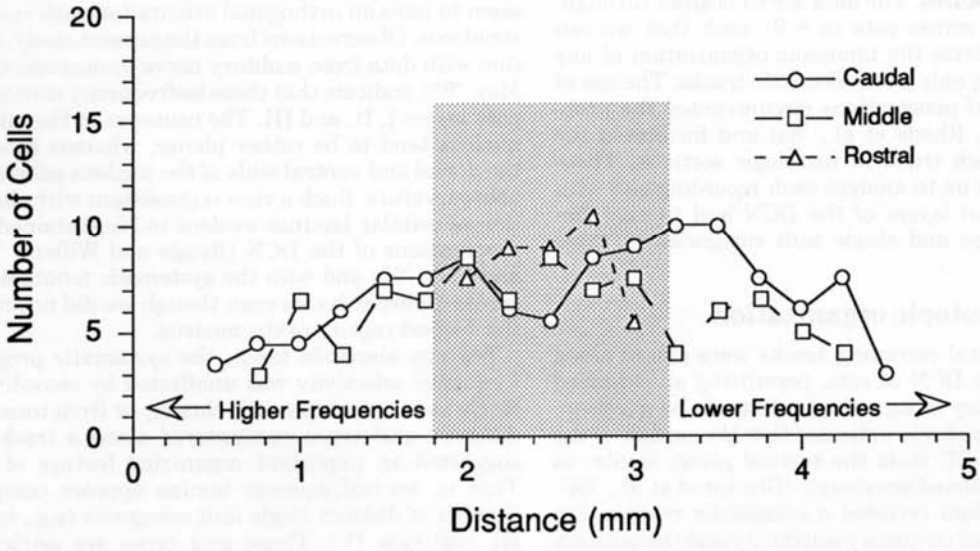

Fig. 11. Distribution and number of HRP-labeled cells from a caudal, 33rd percentile section **(left)** and a rostral, 67th percentile section **(right)**. The computer-aided plots (same scale as in Fig. 10) indicate the relatively uniform labeling in layer II and the less dense labeling in layer III. For each third of the DCN along the rostral-caudal axis, the number of labeled cells in layer II was determined in 0.25 mm bins along the strial axis. Highest cell counts were obtained for bins in the middle third of the nucleus **(shaded area)** along the dorsal-ventral axis. The number of cells in this middle frequency region is further increased relative to high and low frequencies because rostral cells are located exclusively in the middle third of the DCN.

topographically related to the injection site in the inferior colliculus. An injection site in the dorsal region of the inferior colliculus labeled neurons in the more ventral and lateral portion of the DCN, whereas an injection site in the ventral region of the inferior colliculus labeled cells located more dorsally and medially. One HRP case was studied extensively because the injection site covered one entire inferior colliculus and all large neurons in the contralateral DCN appeared to be labeled. Labeled cells with a visible nucleus were counted and their positions plotted on an outline of the tissue section (Figs. 10, 11). Each section was divided into 0.25 mm bins along the strial axis and the number of labeled cells per bin was determined. Sections taken from the caudal, middle, and rostral thirds of the nucleus illustrate cell density along the frequency axis (Figs. 10, 11). Sections were aligned using blood vessels and other anatomic landmarks so that bins of similar horizontal (and thus, frequency) positions were assigned the same number. That is, bin 1 was taken from the dorsomedial tip of the nucleus, bin 9 from the middle of the nucleus, and bin 18 from the ventrolateral tip. Owing to a rostral bulge that extends the middle of the nucleus, only the middle bins were found in all sections. This bulge, complete with its layered organization, extends the 8–30 kHz region of the DCN. The density of cells is fairly constant through the middle regions of the nucleus but falls off towards each end (Fig. 11). As a result, this middle region occupies a relatively larger volume and exhibits a slightly higher density of pyramidal cells. This expanded distribution of pyramidal cells in the 8–30 kHz region may reflect a specialization for processing acoustic information in this frequency range. The functional implication of this frequency representation is discussed below.

DISCUSSION

The present report is based on the confident recovery of 18 individual electrode tracks that traversed relatively long stretches without obvious distortion of the tissue caused by the recording procedures. The data are consistent throughout the DCN and across cats (n = 9) such that we can completely characterize the tonotopic organization of any single nucleus using only a few electrode tracks. The use of a limited number of penetrations circumvented the problem of edema (e.g., Rhode et al., '83) and facilitated the identification of each track in histologic sections. These data also permitted us to analyze each recording site with respect to individual layers of the DCN and to map frequency relationships and single unit categories in three dimensions.

Tonotopic organization

Electrophysiological recording tracks were placed along the long axis of the DCN of cats, permitting an extended sampling of frequency along a single electrode penetration. Our stereotaxic procedures indicated that the surface of the DCN is oriented at 37° from the vertical plane, similar to the value of 45° reported previously (Blackstad et al., '84). The physiological data revealed a systematic relationship between the recorded frequency selectivity and the position of the electrode tip along the strial axis. High frequencies are located dorsomedially with successively lower frequencies located progressively more ventrolaterally. This tonotopic relationship has been described using several techniques, including the use of short (< 2 mm) tracks (Rose et al., '59; Rhode and Smith, '86; Yajima and Hayashi, '89) or surface recordings (Kaltenbach and Lazor, '91), the frequency-specific position of 2-deoxyglucose utilization (Ryan et al., '82), the systematic shift in the location of c-FOS immunohistochemistry in response to different frequencies of pure tone stimulation (Friauf et al., '92), and the topographic projections of HRP-labeled auditory nerve fibers (Ryugo and May, '93). The present data extend this base of knowledge by providing long, uninterrupted recording tracks that cover a greater distance and wider frequency range in the DCN than had been previously reported. By sampling at the shortest possible intervals, we have produced a highly reproducible frequency map at the cellular level whose resolution exceeds that produced by previous methods (e.g., Ryugo and May, '93; Ryan et al., '82; Friauf et al., '92).

Our recording procedure was designed to yield the highest unit density, while simultaneously demonstrating that each record was generated by a different neuron. A sampling interval of 100–150 μm was operationally chosen in order to be certain that different units or unit clusters were featured at each recording site. Criteria for accepting a new recording site included changes in the single unit wave form, in the unit response category, or in the audiovisual characteristics of the evoked response. Recordings from the same single unit or multiple unit cluster can extend over distances of 80–100 μm. Sampling at smaller intervals, for example 25 μm, would yield the same frequency values at 3–5 sequential locations due to contact with the same unit, and generate an artificial "staircase" appearance in the map when a new unit was encountered.

Isofrequency laminae

By connecting points of similar frequencies, isofrequency lines were revealed (Fig. 8). This array of isofrequency lines presumably underlies the tonotopic organization of the DCN. Although the contours curve in complex ways, they seem to have an orthogonal orientation with respect to the strial axis. Observations from the present study, in conjunction with data from auditory nerve projections (Ryugo and May, '93), indicate that these isofrequency contours encompass layers I, II, and III. The contours in the middle of the nucleus tend to be rather planar, whereas those towards the dorsal and ventral ends of the nucleus exhibit considerable curvature. Such a view is consistent with the organization of cellular laminae evident in Nissl-stained histologic preparations of the DCN (Ryugo and Willard, '85; Ryugo and May, '92) and with the systematic tonotopic sequence across different layers even though we did not record from the deepest regions of the nucleus.

For any electrode track, the systematic progression in frequency selectivity was unaffected by recordings from a single unit, a multiple unit cluster, or from tone-hash. The different unit types encountered along a track, however, suggested an important organizing feature of the DCN. That is, an isofrequency lamina appears composed of a number of distinct single unit categories (e.g., type II, type III, and type IV). These unit types are unified by their common frequency selectivity yet diversified by their different response properties which presumably underlie separate roles in acoustic information processing.

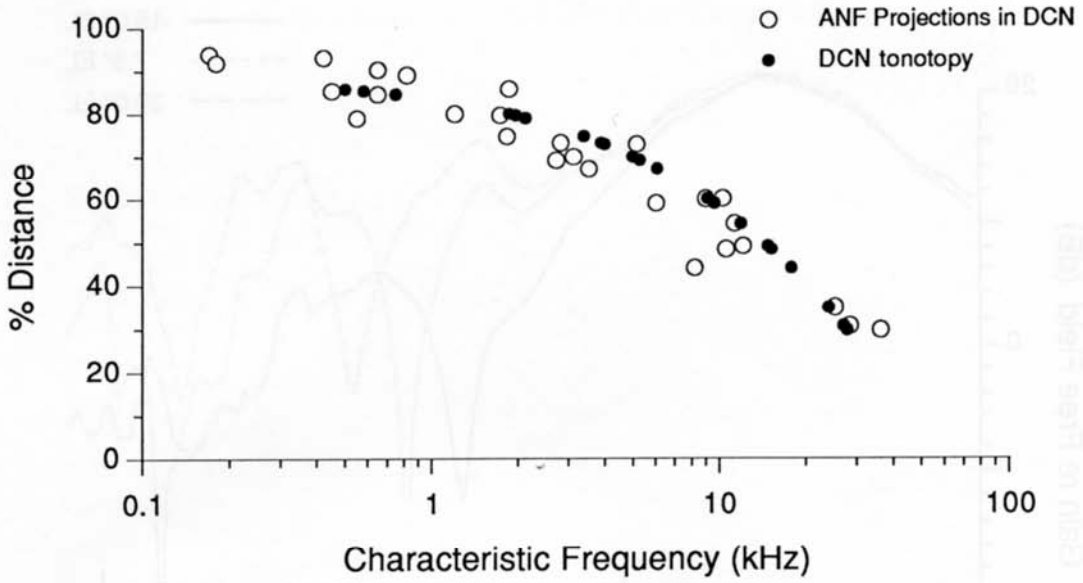

Fig. 12. Distance versus frequency plots for the average of our physiologic data (filled circles) and auditory nerve fiber projections into the DCN from Ryugo and May ('93). Data points for auditory nerve fibers indicate the location of the terminal field for a single fiber with respect to its CF. The similarity of these two plots is consistent with the idea that the tonotopic organization of the DCN is determined by the pattern of auditory nerve projections.

The presence of different unit types is related to the DCN layer in which the recording was made (Table 1). Type IV and "transitional" type IV units (transitional because they have some characteristics of type III units) were found mostly in layers II and III as has been previously reported (Young and Brownell, '76; Shofner and Young, '85). These units have been shown to arise from pyramidal neurons (Rhode et al., '83; Smith and Rhode, '85), the principal DCN cell type having efferent projections in the dorsal acoustic stria (Osen, '70; Adams and Warr, '76; Young, '80; Ryugo and Willard, '85). In the superficial DCN of anesthetized preparations, pyramidal cells most likely generate all of the pauser and build-up responses and many of the chopper responses (Godfrey et al., '75; Rhode et al., '83; Manis, '90). Type III units were found in all layers, and type II units were found exclusively in layer III. Cross-correlational analysis using electrophysiological methods suggests that type II units are synaptically connected to pyramidal neurons within similar frequency ranges (Voigt and Young, '90). Layer I also contained 4 units that exhibited action potentials with multiple peaks. These "complex-spiking" units in the cat had virtually identical wave forms to those intracellularly characterized from layers I and II in DCN slices of the guinea pig brainstem and shown to be cartwheel cells (Spirou et al., '91).

The organization of each isofrequency contour as a tissue slab seems to represent a functional module oriented in the trans-strial dimension. Each module would be comprised of the same cell classes but would differ in the number of the individual cells representing each class. Spanning the depth of any module are the terminal fields of incoming auditory nerve fibers and the cell bodies and dendrites of, for example, pyramidal, giant, granule, Golgi, cartwheel, stellate, and vertical cells. The axonal ramifications of local circuit neurons might also serve to maintain isofrequency relationships (Voigt and Young, '90). Computer-aided anatomical observations of individual cartwheel neurons reveal that each emits a local circuit axon whose arborization is confined to the isofrequency lamina of origin (Manis, Spirou, Wright, Paydar, and Ryugo, unpublished observations). Furthermore, cartwheel cells form synaptic connections with other cartwheel neurons, stellate cells, and pyramidal neurons (Berrebi and Mugnaini, '91). It remains to be determined how other cell categories of the DCN (e.g., vertical cells, giant cells, etc.) are functionally integrated within an isofrequency module and how these interactions shape the output activity of the efferent projections.

Distance versus frequency along the strial axis

The shape of the distance-frequency plot has a characteristic profile such that, on a log frequency scale, the slope of the profile continues to increase with frequency. The slope of the profile in the 20–40 kHz octave range is more than three times the slope in the 2–4 kHz octave range. Thus, the distance covered along the strial axis is much greater for high frequency octaves than for low frequency octaves. This profile, then, differs considerably from that of the cochlea, where the same distance along the cochlear partition is devoted to high versus low frequency octaves (Liberman, '82).

Inhibitory interactions in the DCN are also mostly expressed along the strial dimension (Voigt and Young, '90). That is, the response properties for some cell classes are influenced by near but dissimilar frequency regions, resembling the phenomenon of lateral inhibition. Our derived polynomial function can compute the actual distance between arbitrary isofrequency laminae, thereby calculating the spread of neuronal processes that may account for neural interactions. For example, response

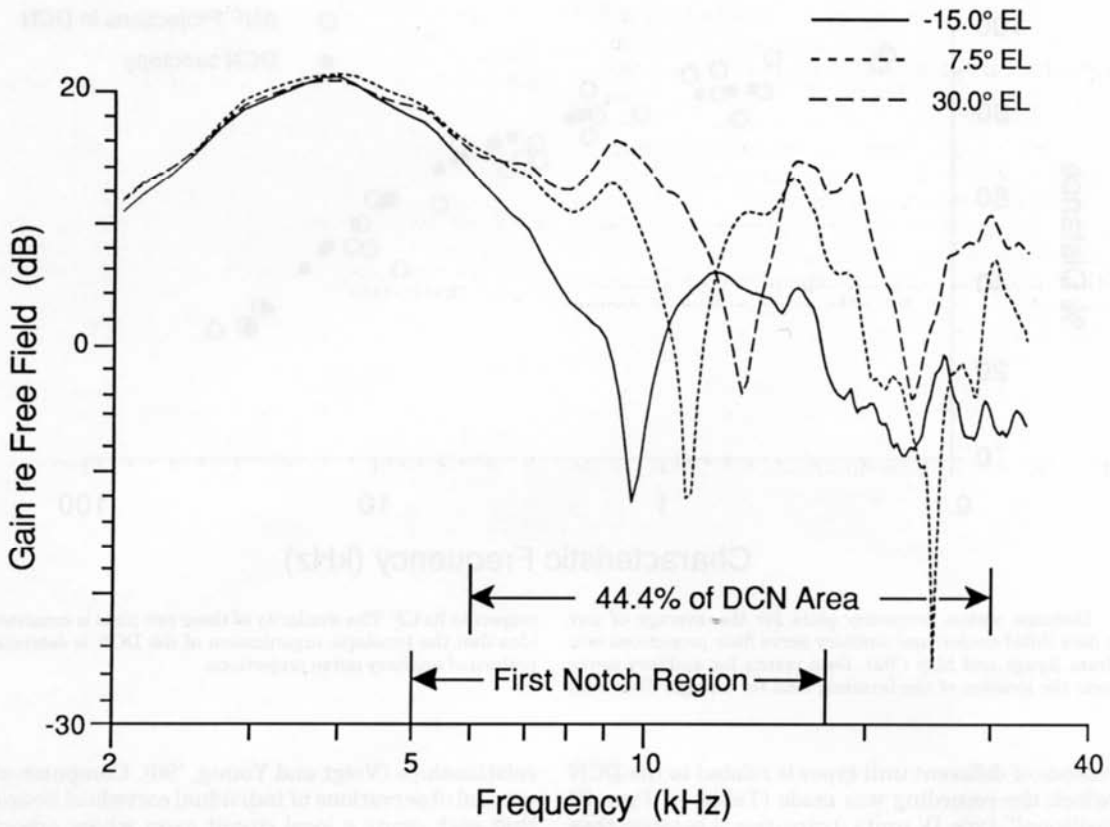

Fig. 13. Effects of a cat's pinna on spectral properties of broad band acoustic stimuli at a constant azimuth (15°), but at three different elevations. Frequencies marked with prominent energy minima (called notches) change with sound direction. The "first notch" (FN) region represents that range of frequencies where notches exhibit the most systematic changes. These frequencies are enhanced by the frequency organization of the DCN. The middle third of the strial axis actually represents 44.4% of the area of the sheet of layer II because of the rostral bulge (figure modified from Rice et al., '92).

maps of type IV units indicate that dominant inhibitory inputs are centered at 0.17 octaves below the CF of the type IV unit (Spirou and Young, '91). This value translates into distances of approximately 85 μm at 5 kHz and 200 μm at 30 kHz along the frequency dimension of the nucleus. Therefore, the axons of local inhibitory neurons, such as for type II units, are hypothesized to traverse these distances in their respective frequency regions.

Auditory nerve projections and DCN tonotopic map

The terminal fields of type I auditory nerve fibers exhibit a systematic relationship between fiber characteristic frequency and DCN location (Ryugo and May, '93). Furthermore, the alignment and orientation of the terminal arborizations corresponds to the striations formed by resident cell bodies in layer III. By normalizing the position of HRP-labeled terminal fields of auditory nerve fibers in the DCN, we can compare the primary projections to the DCN tonotopic map, despite the pooling across different animals and a lack of extremely high frequency examples (Fig. 12). These spatial data are consistent with the idea that the auditory nerve provides the tonotopic organization to the DCN, yet it remains noteworthy that the organization of second-order units exhibits relatively less variability than that observed for the primary input.

Functional implications of the frequency representation

The frequency map constructed from our physiological measures provides an accurate description of the distance along the strial axis that separates particular frequency locations in the DCN of the cat. It does not, however, provide information regarding the frequency representation in dimensions orthogonal to the strial axis (Kaltenbach and Lazor, '91) or the curvature of isofrequency contours in the extreme ends of the nucleus. Owing to the irregular shape of the nucleus, strial distance does not necessarily reflect the volume of tissue or the number of neurons in the DCN devoted to the processing of frequency information. The middle third of the DCN, as calculated along the strial axis, is characterized by the most regular cellular architecture in the nucleus (Blackstad et al., '84) and contains the greatest amount of tissue relative to that of the dorsomedial and ventrolateral regions. This expansion is evident by the rostral bulge in the middle third of the nucleus (see Fig. 8) and by increased pyramidal cell counts (Fig. 11). If layer II is considered to be a two-dimensional sheet formed by a single layer of pyramidal cells having relatively uniform density, then frequencies from 8–30 kHz, which occupy the middle third of the nucleus along the strial axis, encompass nearly half of the total area of layer II.

The expansion of tissue in the DCN devoted to the processing of 8–30 kHz may be interpreted as an anatomical and physiological specialization for the neural processing of spectral cues for sound localization. For example, acoustic measures indicate that the cat's pinna introduces a prominent notch in the middle frequency spectrum of broadband noise (Musicant et al., '90; Rice et al., '92). The spectral notch may serve as an important cue for directional hearing because the frequency location of the notch changes systematically with respect to the location of the source of the noise (Fig. 13). Therefore, the expanded representation of frequencies between 8–30 kHz could reflect a design feature incorporated into the DCN for assisting in the localization of complex sounds. This hypothesis is supported by recent single unit studies which indicate that the response properties of pyramidal cells in the cat DCN are well suited for the neural encoding of spectral notches (Young et al., '92) and by behavioral studies which indicate sound localization based on spectral cues is disrupted by surgical ablation of the ascending pathway of the DCN (Sutherland and Masterton, '92).

ACKNOWLEDGMENTS

This work was supported in part by NIH grants DC00232, DC00115, and NS08333. We thank C.M. Aleszczyk, T. Pongstaporn, and P.P. Taylor for their technical assistance. We also thank Dr. E.D. Young and Dr. M.B. Sachs for making their recording facilities available to us. Portions of these data have been presented in abstract form at the 19th Annual Meeting for the Society for Neuroscience and at the 14th Midwinter Meeting of the Association for Research in Otolaryngology.

LITERATURE CITED

Adams, J.C. (1979) Ascending projections to the inferior colliculus. J. Comp. Neurol. *183:*519–538.

Adams, J.C., and W.B. Warr (1976) Origins of axons in the cat's acoustic striae determined by injection of horseradish peroxidase into severed tracts. J. Comp. Neurol. *170:*107–121.

Aitkin, L.M., and W.R. Webster (1972) Medial geniculate body of the cat: Organization and responses to tonal stimuli of neurons in ventral division. J. Neurophysiol. *35:*365–380.

Bekesy, G. von (1960) Experiments in Hearing (translated and edited by E.G. Wever). New York: McGraw-Hill Book Co.

Berrebi, A.S., and E. Mugnaini (1991) Distribution and targets of the cartwheel cell axon in the dorsal cochlear nucleus of the guinea pig. Anat. Embryol. *183:*427–454.

Blackstad, T.W., K.K. Osen, and E. Mugnaini (1984) Pyramidal neurones of the dorsal cochlear nucleus: A Golgi and computer reconstruction study in cat. Neuroscience *13:*827–854.

Bruns, V., and E. Schmieszek (1980) Cochlear innervation in the greater horseshoe bat: Demonstration of an acoustic fovea. Hearing Res. *3:*27–43.

Clopton, B.M., J.A. Winfield, and F.J. Flammino (1974) Tonotopic organization: Review and analysis. Brain Res. *76:*1–20.

Evans, E.F., and P.G. Nelson (1973) The responses of single neurones in the cochlear nucleus of the cat as a function of their location and the anesthetic state. Exp. Brain Res. *17:*402–427.

Friauf, E., K. Kandler, and F. Weber (1992) Cell birth, formation of efferent connections and establishment of tonotopic order in rat cochlear nucleus. In The Mammalian Cochlear Nuclei: Organization and Function M.A. Merchan, J.M. Juiz, and D.A. Godfrey (eds): New York: Plenum Press.

Godfrey, D.A., N.Y.S. Kiang, and B.E. Norris (1975) Single unit activity in the dorsal cochlear nucleus of the cat. J. Comp. Neurol. *162:*269–284.

Guinan, J.J., B.E. Norris, and S.S. Guinan (1972) Single auditory units in the superior olivary complex. II. Locations of unit categories and tonotopic organization. Intern. J. Neurosci. *4:*147–166.

Heffner, R.S., and H.E. Heffner (1985) Hearing range of the domestic cat. Hearing Res. *19:*85–88.

Kaltenbach, J.A., and J. Lazor (1991) Tonotopic maps obtained from the surface of the dorsal cochlear nucleus of the hamster and rat. Hearing Res. *51:*149–160.

Konishi, M. (1986) Centrally synthesized maps of sensory space. Trends Neurosci. *9:*163–168.

Liberman, M.C. (1982) The cochlear frequency map for the cat: Labeling auditory-nerve fibers of known characteristic frequency. J. Acoust. Soc. Am. *72:*1441–1449.

Manis, P.B. (1990) Membrane properties and discharge characteristics of guinea pig dorsal cochlear nucleus neurons studied *in vitro*. J. Neurosci. *10:*2338–2351.

Masterton, R.B., G.C. Thompson, J.K. Bechtold, and M.J. RoBards (1975) Neuroanatomical basis of binaural phase-difference analysis for sound localization: A comparative study. J. Comp. Physiol. Psych. *89:*379–386.

May, B.J., C.M. Aleszczyk, and M.B. Sachs (1991) Single-unit recording in the ventral cochlear nucleus of behaving cats. J. Neurosci. Methods *40:*155–169.

Merzenich, M.M., and M.D. Reid (1974) Representation of the cochlea within the inferior colliculus of the cat. Brain Res. *77:*397–415.

Musicant, A.D., J.C.K. Chan, and J.E. Hind (1990) Direction-dependent spectral properties of cat external ear: New data and cross-species comparisons. J. Acoust. Soc. Am. *87:*757–781.

Osen, K.K. (1969) Cytoarchitecture of the cochlear nuclei in the cat. J. Comp. Neurol. *136:*453–484.

Osen, K.K. (1970) Course and termination of the primary afferents in the cochlear nuclei of the cat. Arch. Ital. Biol. *108:*21–51.

Pollak, G.D. (1989) The functional organization of the auditory brainstem in the mustache bat and mechanisms for sound localization. In R.N. Singh and N.J. Strausfeld (eds): Neurobiology of Sensory Systems New York: Plenum Publishing Corp., pp. 469–497.

Rhode, W.S., and P.H. Smith (1986) Physiological studies on neurons in the dorsal cochlear nucleus of cat. J. Neurophysiol. *56:*287–307.

Rhode, W.S., P.H. Smith, and D. Oertel (1983) Physiological response properties of cells labeled intracellularly with horseradish peroxidase in cat dorsal cochlear nucleus. J. Comp. Neurol. *213:*426–447.

Rice, J.J., B. May, G.A. Spirou, and E.D. Young (1992) Pinna-based spectral cues for sound localization in cat. Hearing Res. *58:*132–152.

Rose, J.E., R. Galambos, and J.R. Hughes (1959) Microelectrode studies of the cochlear nuclei of the cat. Bull. Johns Hopkins Hospital *104:*211–251.

Ryan, A.F., N.K. Woolf, and F.R. Sharp (1982) Tonotopic organization of the central auditory pathway of the mongolian gerbil: A 2-deoxyglucose study. J. Comp. Neurol. *207:*369–380.

Ryugo, D.K., and S.K. May (1993) The projections of intracellularly labeled auditory nerve fibers to the dorsal cochlear nucleus of cats. J. Comp. Neurol. *329:*20–35.

Ryugo, D.K., and F.H. Willard (1985) The dorsal cochlear nucleus of the mouse: A light microscopic analysis of neurons that project to the inferior colliculus. J. Comp. Neurol. *242:*381–396.

Shofner, W.P., and E.D. Young (1985) Excitatory/inhibitory response types in the cochlear nucleus: Relationships to discharge patterns and responses to electrical stimulation of the auditory nerve. J. Neurophysiol. *54:*917–939.

Smith, P.H., and W.S. Rhode (1985) Electron microscopic features of physiologically characterized, HRP-labeled fusiform cells in the cat dorsal cochlear nucleus. J. Comp. Neurol. *237:*127–143.

Sokolich, W.G. (1977) Improved acoustic system for auditory research. J. Acoust. Soc. Am. *62:*S12.

Spirou, G.A., and E.D. Young (1991) Organization of dorsal cochlear nucleus type IV unit response maps and their relationship to activation by bandlimited noise. J. Neurophysiol. *66:*1750–1768.

Spirou, G.A., D.D. Wright, D.K. Ryugo, and P.B. Manis (1991) Physiology and morphology of cells from slice preparations of the guinea pig dorsal cochlear nucleus. Abst. Assn. Res. Otolaryngol. *14:*142.

Suga, N. (1988) Auditory neuroethology and speech processing: Complex-sound processing by combination-sensitive neurons. In G.M. Edelman, W.E. Gall, and W.M. Cowan (eds): Auditory Function. New York: John Wiley and Sons, pp. 679–720.

Sutherland, D.P., and R.B. Masterton (1992) Effect of unilateral lesions on discrimination of changes in sound source elevation. Abstr. Assn. Res. Otolaryngol. *15:*51.

Voigt, H.F., and E.D. Young (1990) Cross-correlation analysis of inhibitory interactions in dorsal cochlear nucleus. J. Neurophysiol. *64:*1590–1610.

Woolsey, C.N. (1960) Organization of cortical auditory system: A review and synthesis. In G.L. Rasmussen and W.F. Windle (eds): Neural Mechanisms of the Auditory and Vestibular Systems. Springfield: Charles C. Thomas Publishers, pp. 165–180.

Yajima, Y., and Y. Hayashi (1989) Response properties and tonotopical organization in the dorsal cochlear nucleus in rats. Exp. Brain Res. *75:*381–389.

Young, E.D. (1980) Identification of response properties of ascending axons from dorsal cochlear nucleus. Brain Res. *200:*23–37.

Young, E.D., and W.E. Brownell (1976) Responses to tones and noise of single cells in dorsal cochlear nucleus of unanesthetized cats. J. Neurophysiol. *39:*282–300.

Young, E.D., G.A. Spirou, J.J. Rice, and H.F. Voigt (1992) Neural organization and responses to complex stimuli in the dorsal cochlear nucleus. Phil. Trans. R. Soc. London B *336:*407–413.